Neuron, Volume *109*

Supplemental information

Locus coeruleus anchors a trisynaptic circuit controlling fear-induced suppression of feeding

Ben Yang, Javier Sanches-Padilla, Jyothisri Kondapalli, Sage L. Morison, Eric Delpire, Rajeshwar Awatramani, and D. James Surmeier

Fig. S1 - Yang et al.

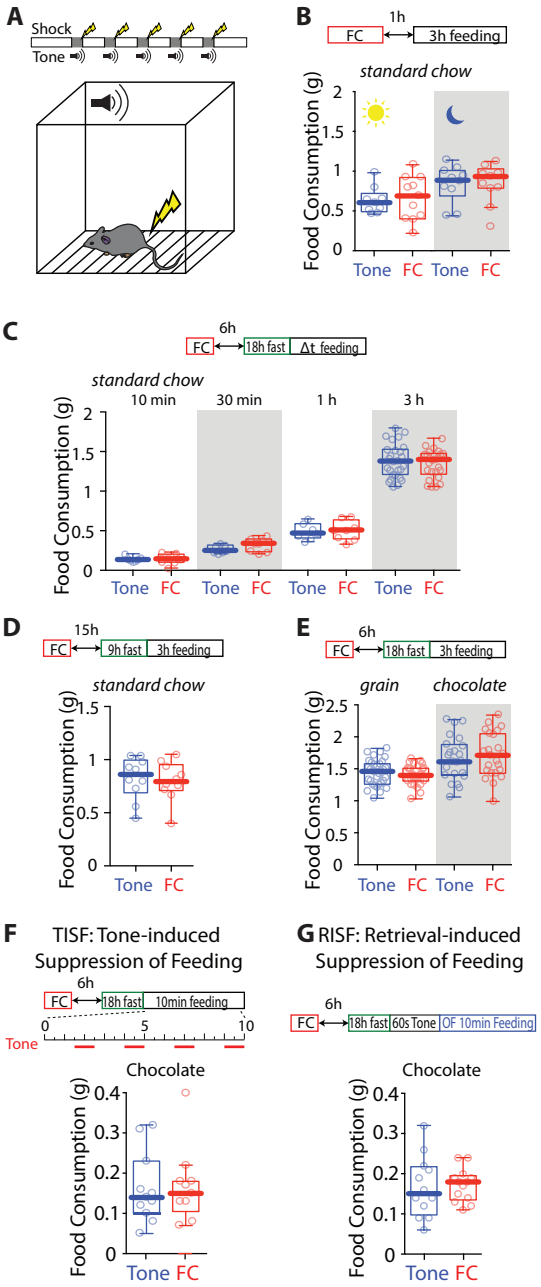

Figure S1. Fear conditioning *per se* did not affect feeding, related to Figure 1.

(A) Cartoon showing fear conditioning protocol.

(B-G) Upper: fear conditioning and feeding protocols; Lower:

(B) Free feeding: Fear conditioned (FC) mice consumed a similar amount of chow as control mice treated with tone alone (Tone) both during the day (left) and night (right).

(C-E) Fasting and feeding: FC and Tone mice consumed a similar amount of chow after 18-hours fasting (C) and 9-hours fasting (D), a similar amount of precision pellets after 18-hours of fasting (E).

(F-G) FC mice consumed a similar amount of chocolate pellets during (G) and after (H) fear memory retrieval.

Statistics: n.s. $p > 0.05$, Mann-Whitney U test. Also see Table S1.

Fig. S2 - Yang et al.

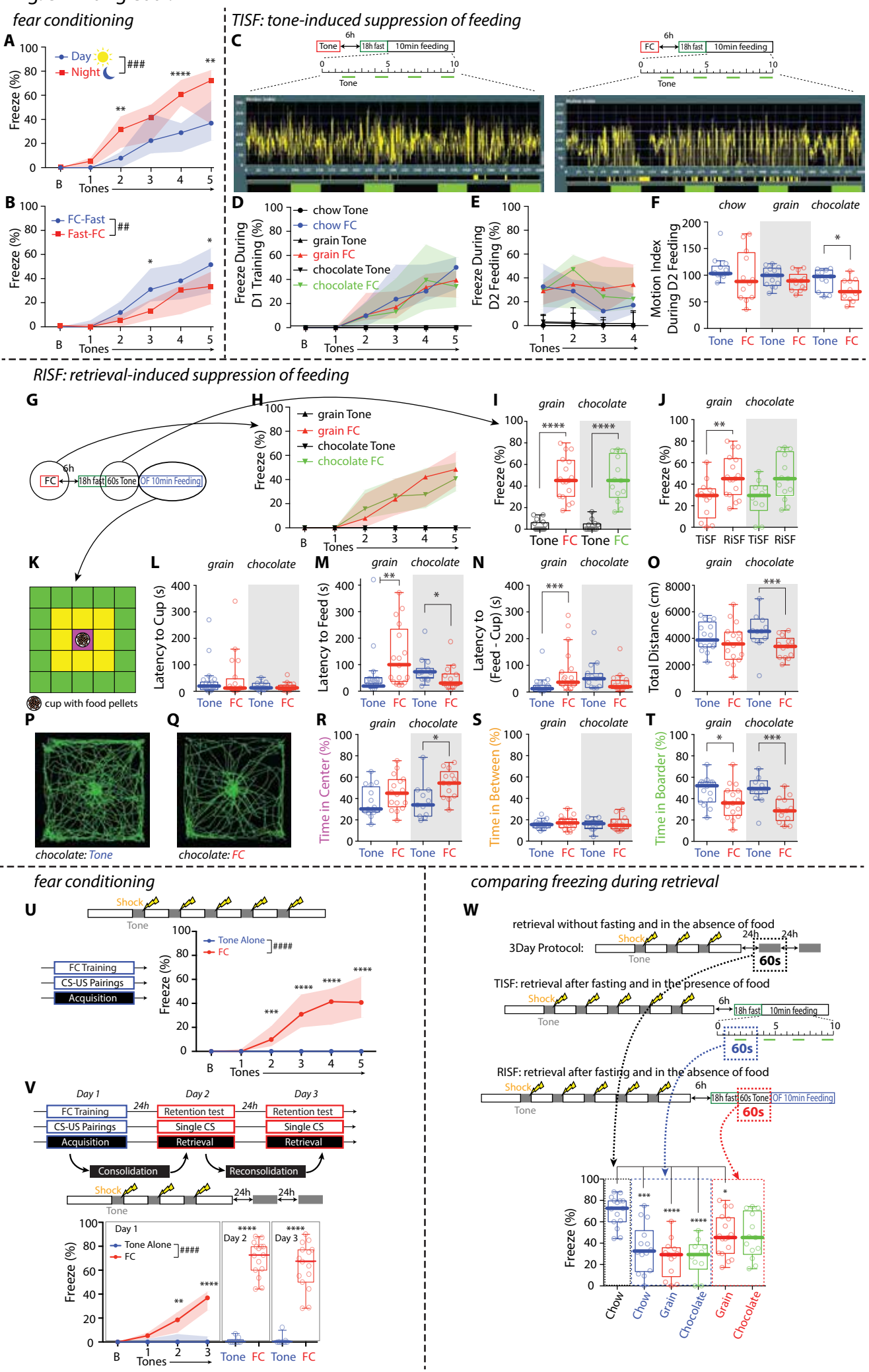

Figure S2. Behavioral analysis of fear conditioning and feeding, related to Figure 1 & S1

(A-B) Circadian clock and homeostatic state affected fear learning.
(A) Mice showed higher freezing level at night than at day during fear-conditioning training.
(B) Fasted mice showed less freezing during fear-conditioning training.
(C-F) Behavioral analysis of tone-induced suppression of feeding (TISF).
(C) Examples of Motion Index (yellow traces in the upper part of figures) and freezing (yellow vertical lines in the middle of figures) analysis of FC and Tone mice during feeding in the presence of tones (green bars in the bottom of figures).
(D-E) Freezing levels during fear memory acquisition (D) and retrieval when mice were feeding (E).
(F) Average motion index during TISF.
(G-T) Behavioral analysis of retrieval-induced suppression of feeding (RISF).
(G) Diagram of the protocol.
(H-I) The freezing levels during fear memory acquisition (H) and retrieval (I).
(J) Freezing during fear memory retrieval with (TISF, historical data in E first tone) and without (RISF, historical data in I FC) the presence of food. The presence of food reduced freezing during fear memory retrieval.
(K) Open field arena with food cup in the middle and different zones colored differently.
(L-N) Latency to the cup (L), feed (M), and (feed-cup) (N) showing that FC mice spent more time to initiate grain, but not chocolate pallets, feeding than Tone mice in RISF after fear memory retrieval.
(O) Total distance traveled during RISF in the open field arena.
(P-Q) Examples of path data of Tone (P) and FC (Q) mice during RISF with chocolate pellets.
(R-T) Percentage of time spent in each zones of the open field showing FC mice spent more time in the center (R) and less in the boarder (T) especially when chocolate is provided.
(U-V) Freezing during fear conditioning and retrieval. Upper: Schematic illustration of 1 day (U) and 3 days (V) fear conditioning protocols; lower: mice treated with fear-conditioning showed significantly higher freezing than treated with tone alone.
(W) Upper: Schematic illustration of the protocols; lower: freezing during retrieval is significantly lower after fasting with (blue, historical data in E first tone) or without (red, historical data in I FC) the presence of food than in non-fasted mice (black, historical data in V day 2 FC).
Statistics: * $p \leq 0.05$, ** $p \leq 0.005$, *** $p \leq 0.001$, **** $p \leq 0.0001$, ## $p \leq 0.005$, ### $p \leq 0.001$; #### $p \leq 0.0001$. Two-way ANOVA with Bonferroni's multiple comparisons (A, B, D, E, H, U-V), Mann-Whitney U test (F, I, J, L-O, R-T, W). Also see Table S1.

Fig. S3 - Yang et al.

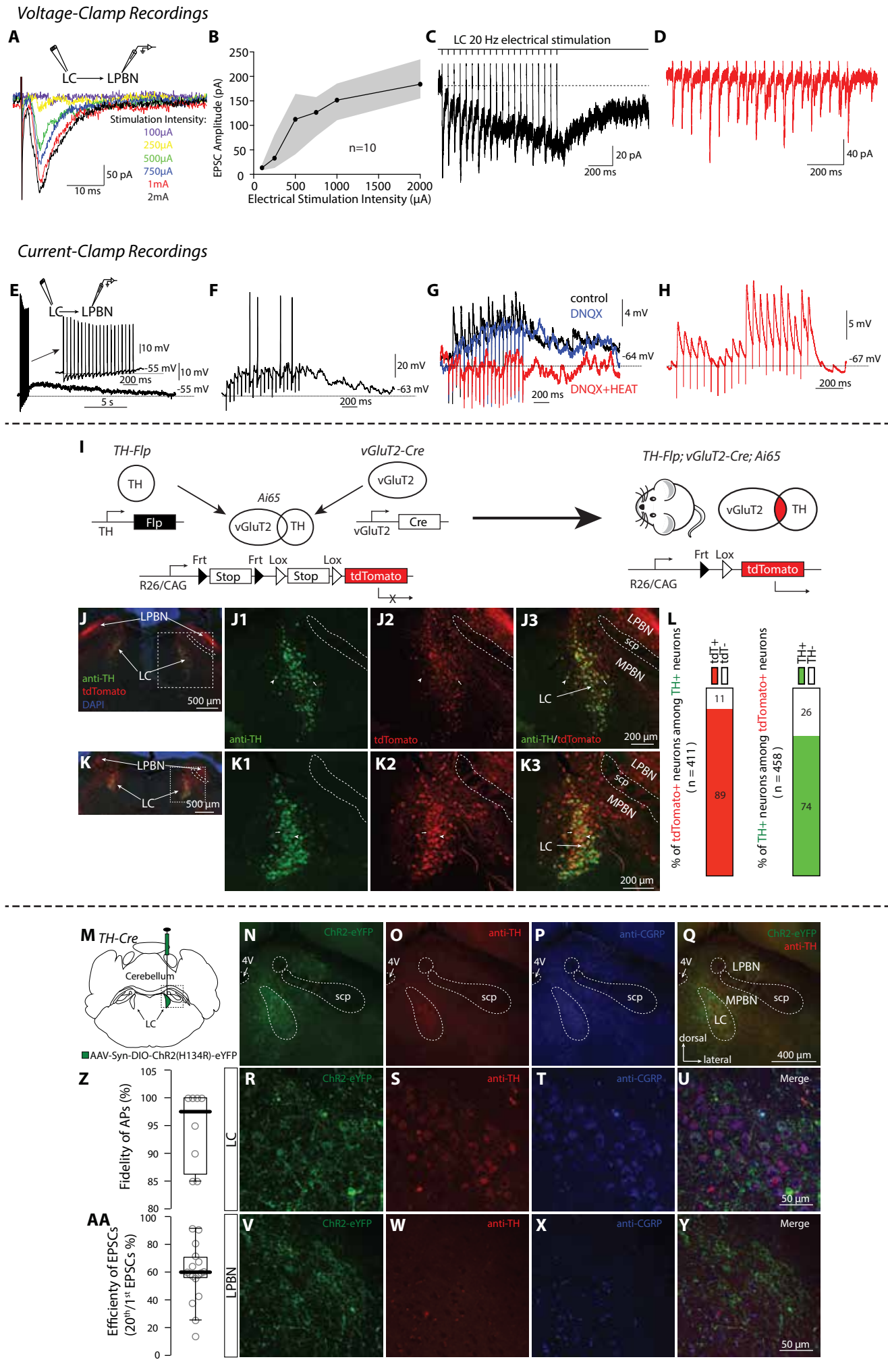

Figure S3. Related to Figure 2

Upper: Recordings of LC excitatory input to PBN. Electrical stimulation of LC evoked both EPSCs and PIC in voltage-clamp recordings (A-D), EPSPs and persistent depolarization potential (PDP) in current-clamp recordings (E-H) in lateral PBN neurons.

(A) Recordings of EPSCs in lateral PBN neurons with electrical stimulation of LC.

(B) Average LC-induced EPSCs in WT naïve mice (n = 10, N = 2).

(C) Example recording showing both EPSCs and PIC (persistent inward current) in a lateral PBN neuron upon 20 Hz electrical stimulation of LC.

(D) When the electrode was placed rostrodorsal to LC (see Figure S5A), 20Hz stimulation induced only EPSCs but no PIC in PBN neurons.

(E-G) 20Hz electrical stimulation of LC induced action potentials and/or EPSPs with PDP (persistent depolarization potential) in PBN neurons.

(H) When the electrode was placed rostrodorsal to LC (see Figure S5A), 20Hz stimulation induced only EPSPs but no PDP in PBN neurons.

Middle and Lower: LC neurons expression of vGlut2 and release of glutamate.

(I) Triple crossing for the generation of *TH-Flp;vGlut2-Cre;Ai65* mice in which tdTomato is expressed only in TH and vGlut2 double-positive cells.

(J-K) Brain slices from *TH-Flp;vGlut2-Cre;Ai65* mice containing the LC showed expression of tdTomato in LC neurons. In J1-3 and K1-3, the small arrow labeled a LC neuron that expresses tdTomato but not TH, the small arrowhead labeled a LC neuron that expresses TH but not tdTomato.

(L) Summary of percentage of tdTomato+ and TH-IR+ cells.

(M) Injection of AAV-EF1α-DIO-ChR2-eYFP into the LC of *TH-cre* mice.

(N-Y) TH and CGRP immunostaining of brain slices from M showing expression of ChR2 in LC neurons and LC fibers in lateral PBN. Note: in R-U most of LC neurons expressed both TH and CGRP while in V-Y only very few lateral PBN neurons expressed TH and a subpopulation expressed CGRP.

(Z) Summary of fidelity of action potentials (APs) in LC neurons expressing ChR2 upon 20Hz optical stimulation (n = 8, median: 97.5%).

(AA) Summary of efficiency of EPSCs (% of $20^{th}/1^{st}$ EPSCs) recorded in lateral PBN neurons upon 20Hz optical stimulation of LC neurons expressing ChR2 (n = 17, median: 59.9%)

Fig. S4 - Yang et al.

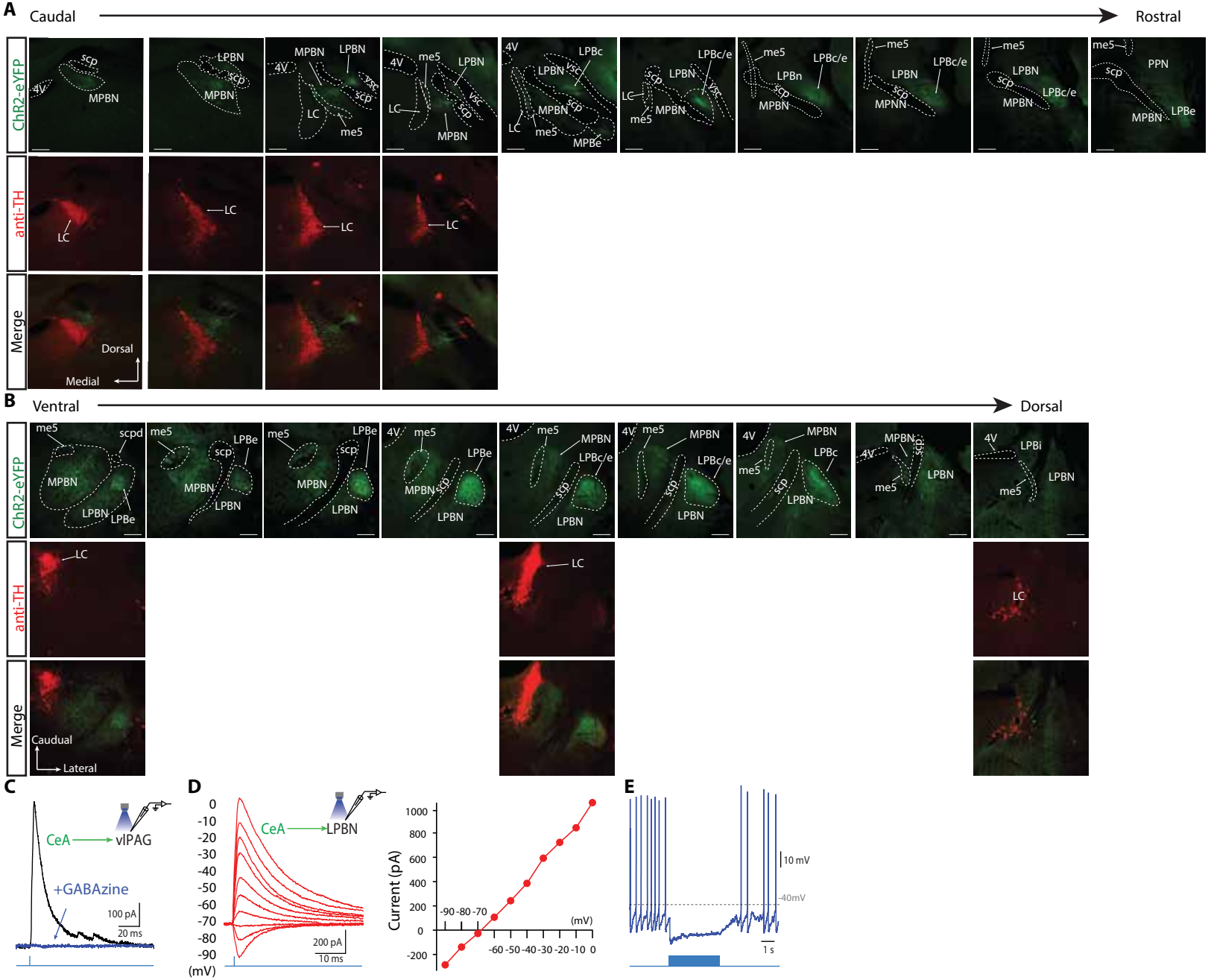

Figure S4. Terminal projections of CeA expressing ChR2(H134R)-eYFP and recordings in vlPAG and LPBN, related to Figure 3.

(A-B) Coronal (A) and horizontal (B) section of LC and PBN in mice injected with AAV-ChR2(H134R)-eYFP into CeA.

(C) IPSC recorded in vlPAG (held at -70 mV) with optical stimulation of CeA terminal expressing ChR2.

(D) IPSCs recorded in lateral PBN (held at -90 to 0 mV) with optical stimulation of CeA terminal expressing ChR2 (right) and I/V curve generated based on these data (left).

(E) Continuous optical stimulation of CeA terminals silenced PBN firing induced with current injection.

LC: locus coeruleus, MPBN: medial parabrachial nucleus, MPBe: external part of the medial parabrachial nucleus, LPBN: lateral parabrachial nucleus, LPBe: external part of the lateral parabrachial nucleus, LPBi: internal part of the lateral parabrachial nucleus, me5: mesencephalic trigeminal tract, scp: superior cerebellar peduncle, scpd: descending limb of the superior cerebellar peduncle, 4V: fourth ventricle, vsc: ventral spinocerebellar tract, PPN: pedunculopontine nucleus. Scale bars: 200 μM, applies to all images.

Fig. S5 - Yang et al.

Electrical stimulation out of LC failed to induce LTD

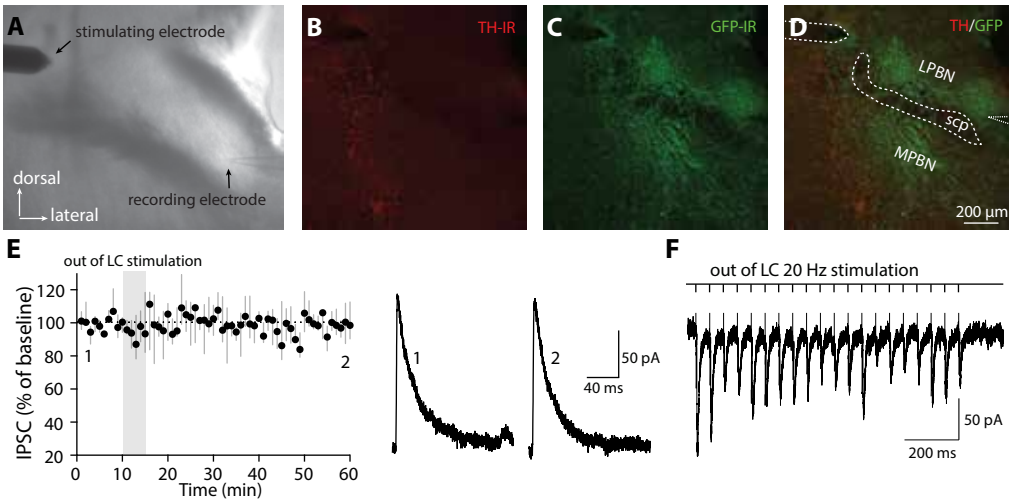

Antagonizing both mGluRs and a1ARs blocked LC stimulation-induced LTD

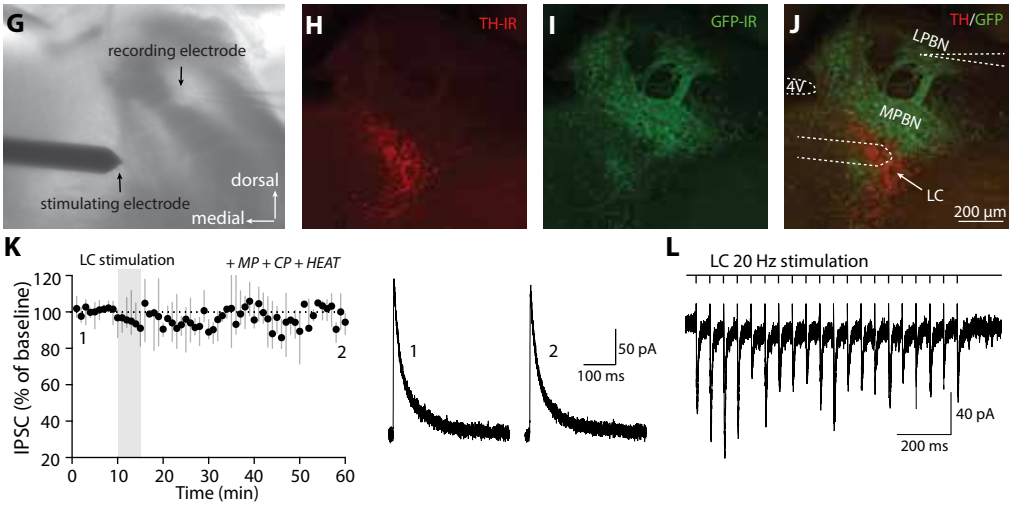

Figure S5. Antagonizing both α1ARs and mGluRs-I blocked LTD at CeA synapses on PBN induced by electrical stimulation of LC, related to Figure 5.

(A-D) Images show electrical stimulation out of the LC while recording a lateral PBN neuron. CeA fibers expressing ChR2-eYFP were stained with anti-GFP antibody after recording.

(E-F) 20Hz electrical stimulation out of the LC induced EPSCs (F) in lateral PBN neurons, but failed to induce LTD (E) of CeA IPSCs (n = 4, N = 3).

(G-J) Images show electrical stimulation of the LC while recording a lateral PBN neuron. CeA fibers expressing ChR2-eYFP were stained with anti-GFP antibody after recording.

(K-L) The combination of mGluRs-I antagonist (MP+CP) and α1ARs antagonist (HEAT) blocked LTD (L) and PIC (L) induced at CeA synapses on PBN upon 20Hz electrical stimulation of LC (n = 4, N = 4).

Fig. S6 - Yang et al.

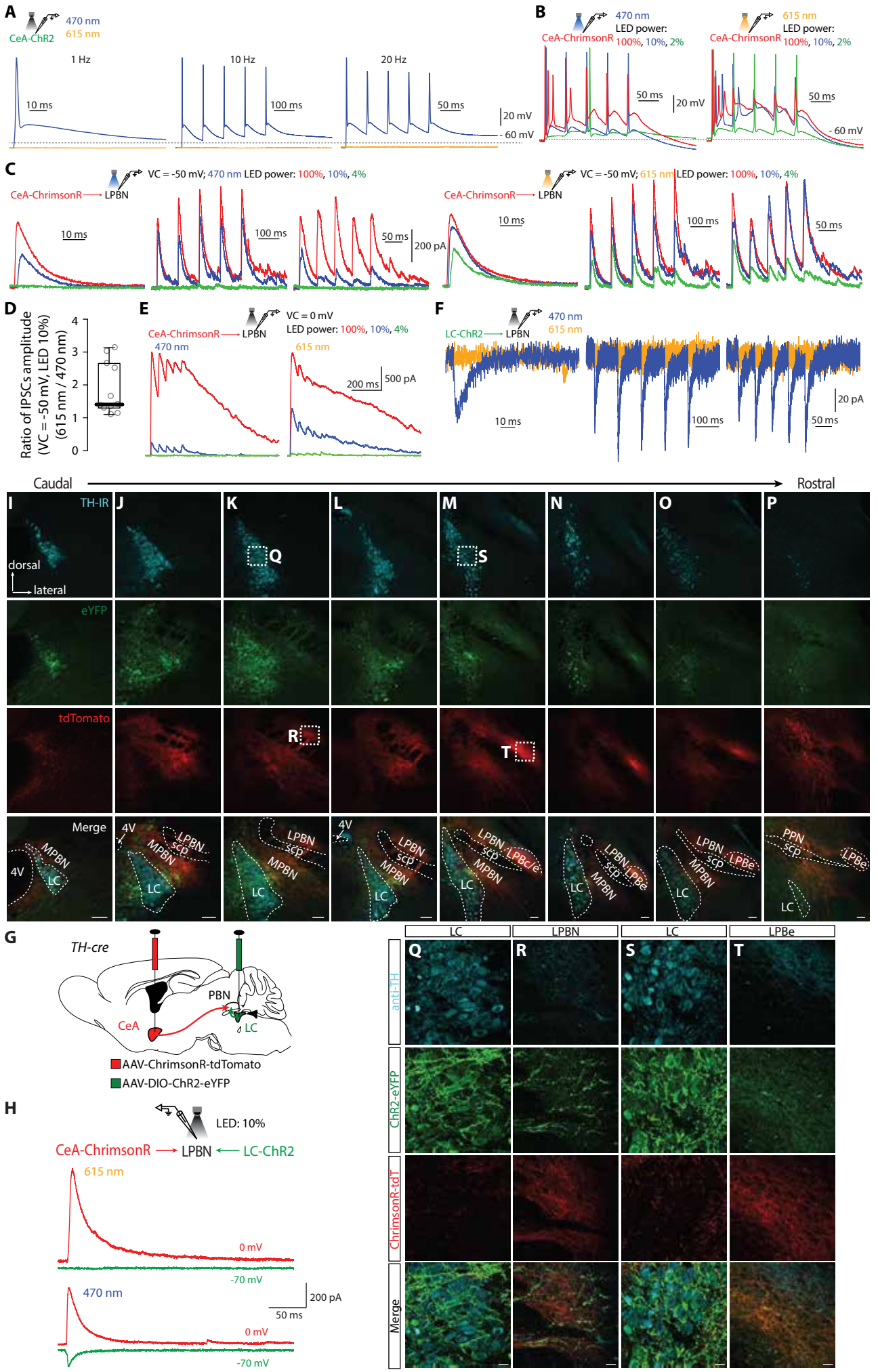

Figure S6. Dual opsins strategy for the recording of both CeA-IPSCs and LC-EPSCs in PBN neurons, related to Figure 5.

(A) Current-clamp recordings of CeA neurons expressing ChR2 when optically stimulated with 470 nm or 615 nm LEDs showing action potentials only with 470 nm LED stimulation.
(B) Current-clamp recordings of CeA neurons expressing ChrimsonR when optically stimulated with 470 nm or 615 nm LEDs showing action potentials with both LEDs stimulation, but more robust with 615 nm LED.
(C, E) Voltage-clamp recordings (-50 mV in C and 0 mV in E) of lateral PBN neurons when optically stimulating CeA-ChrimsonR fibers in the PBN with 470 nm or 615 nm LEDs showing IPSCs with both LEDs stimulation, but more robust with 615 nm LED.
(D) The ratio of IPSCs amplitude when CeA neurons expressing ChrimsonR were voltage-clamped at -50 mV and stimulated with 10% of LED intensity at 615 nm over 470 nm showing ChrimsonR was preferentially activated with 615 nm wavelength.
(F) Voltage-clamp recordings (-70 mV) of lateral PBN neurons when optical stimulating LC-ChR2 fibers in the PBN with 470 nm or 615 nm LEDs showing EPSCs only with 470 nm LED stimulation.
(G) Injection of AAV-Syn-ChrimsonR-tdTomato into the CeA and AAV-EF1α-DIO-ChR2-eYFP into the LC of *TH-cre* mice.
(H) Recordings of CeA-IPSCs with 615 nm LED stimulation and both CeA-IPSCs and LC-EPSCs with 470 nm LED stimulation.
(I-P) Expression of ChR2-eYFP in LC, LC-eYFP fibers and CeA-tdTomato fibers converge in PBN.
(Q-T) Enlarged images of LC and lateral PBN.
LC: locus coeruleus, MPBN: medial parabrachial nucleus, LPBN: lateral parabrachial nucleus, LPBe: external part of the lateral parabrachial nucleus, LPBc/e: central and external part of the lateral parabrachial nucleus, scp: superior cerebellar peduncle, 4V: fourth ventrical, PPN: pedunculopontine nucleus. Scale bars: 100 μM in I-P, 20 μm in Q-T.

Fig. S7 - Yang et al.

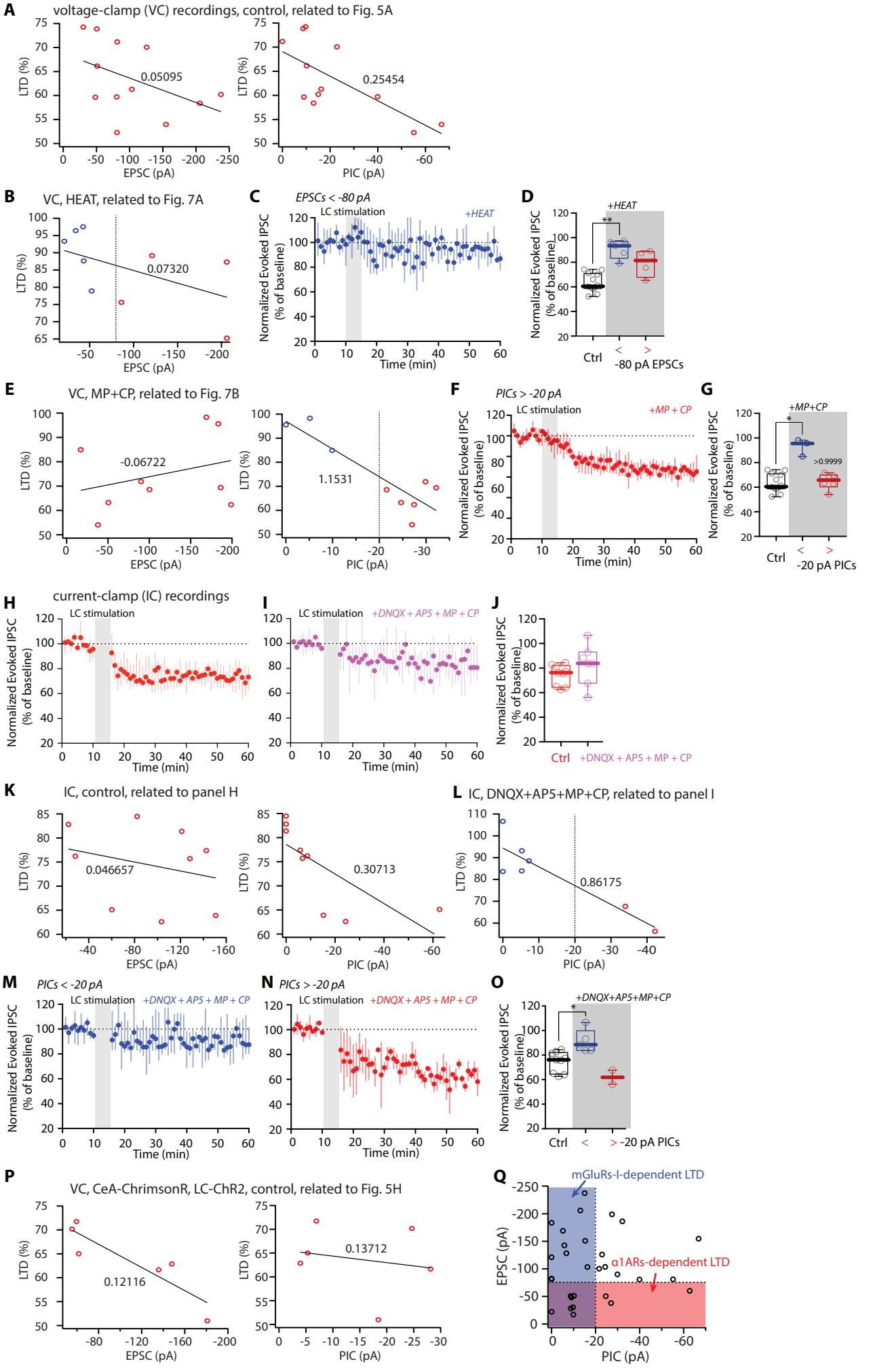

Figure S7. Noradrenaline and glutamate co-released by LC synergized LTD at CeA synapses on lateral PBN, related to Figure 5, 7.

All scatter plots (A, B, C, E, K, L, P). Positive correlations of both EPSC and PIC amplitude with LTD induction. Curve fittings with y = ax + b were shown in solid lines, slope a values were written next by the solid lines. Dash lines in B, E, L, were arbitrary thresholds (-80 pA for EPSC and -20 pA for PIC).

(C) α1ARs antagonist HEAT blocked LTD of CeA-IPSCs in PBN neurons with LC-EPSCs smaller than -80 pA.

(D) Summary of Figures 5A, 7G, S7C.

(F) mGluRs-I antagonists MPEP and CPCCOEt (MP+CP) failed to block LTD of CeA-IPSCs in PBN neurons with LC-PICs bigger than -20 pA.

(G) Summary of Figures 5A, 7F, S7F.

(H-J) In current-clamp recordings, 20Hz electrical stimulation of LC induced LTD of CeA-IPSCs (H), which was not blocked by the combination of DNQX (5 μM), AP5 (50 μM), MPEP (10 μM), and CPCCOEt (25 μM) (DNQX + AP5 + MP+CP, I). Summary in J.

(M-N) iGluRs antagonists and mGluRs-I antagonists (DNQX+AP5+MP+CP) blocked LTD of CeA-IPSCs in PBN neurons with LC-PICs smaller than -20 pA (M), but failed to block LTD in PBN neurons with LC-PICs bigger than -20 pA (N).

(O) Summary of Figures S7H, S7M, S7N.

(Q) Scatter plot of EPSCs and PICs in all PBN neurons. In cells with PICs smaller than -20 pA (blue), activation of mGluRs-I is required for LTD induction; in cells with EPSCs smaller than -80 pA (red), activation of α1ARs is required for LTD induction; in cells with both PICs smaller than -20 pA and EPSCs smaller than -80 pA (blue and red overlaps), both mGluRs-I and α1ARs activations are required for LTD induction; in cells with both PICs bigger than -20 pA and EPSCs bigger than -80 pA (white), either mGluRs-I or α1ARs activations is sufficient for LTD induction. Statistics: * $p \leq 0.05$, ** $p \leq 0.005$, Kruskal Wallis with Dunn's correction. Also see Table S1.

Fig. S8 - Yang et al.

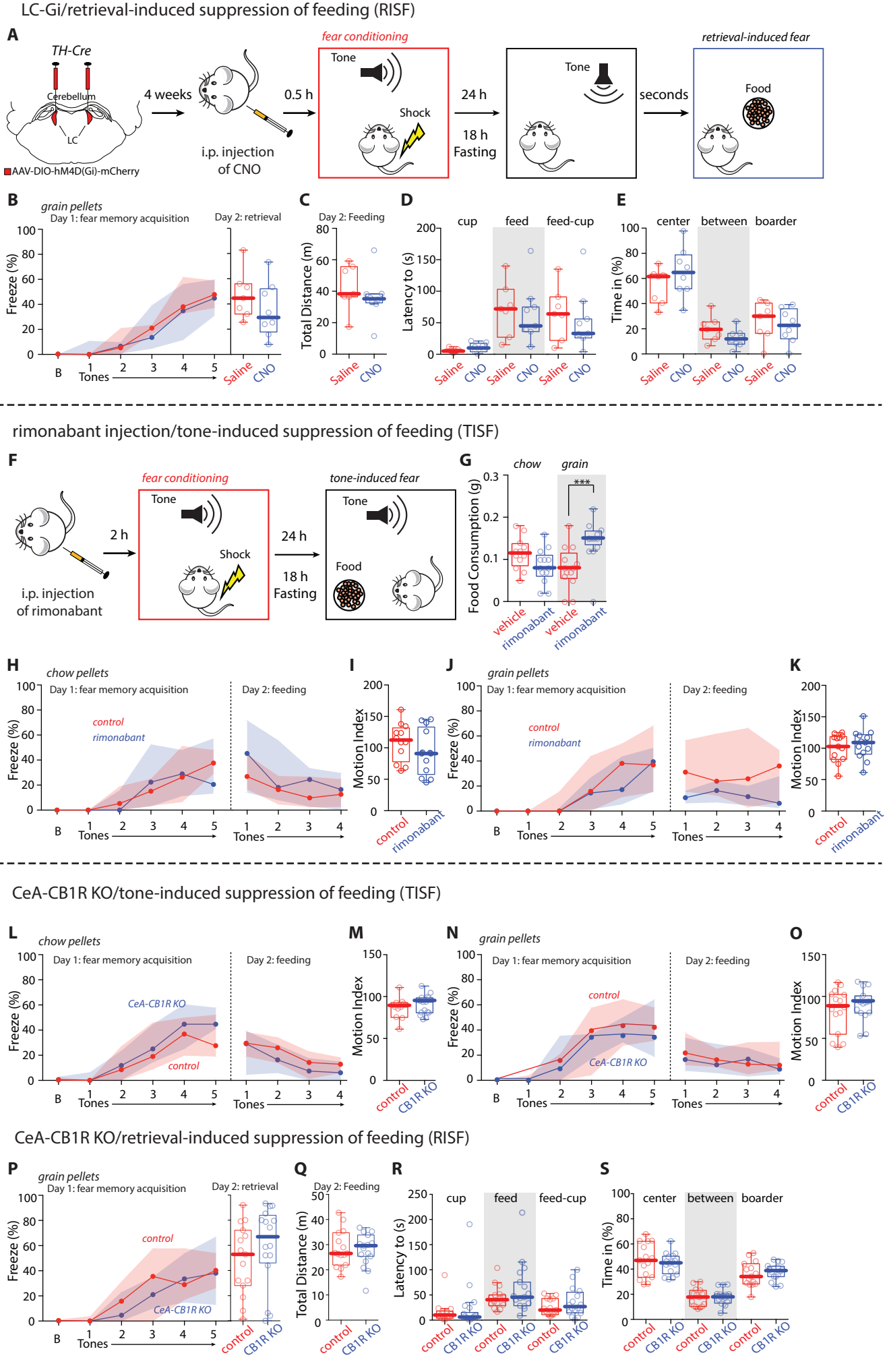

Figure S8. Behavioral analysis of RISF with silencing of LC firing (upper panel); effect of rimonabant on TISF (middle panel); behavioral analysis of TISF and RISF in CeA-CB1R knockdown animals (lower panel), related to Figure 8.

(A) Cartoons showing Gi expression in LC neurons, silencing of LC neurons during fear conditioning and RISF test.
(B) Freezing during fear memory acquisition (left) and retrieval before feeding (right).
(C) Total distance traveled in the open field during feeding.
(D) Latency to reach to cup (left), initial feeding (middle) and (feed - cup) (right).
(E) Percentage of time spent in each zones of the open field during feeding.
(F) Cartoons showing rimonabant injection, fear conditioning, and feeding.
(G) Rimonabant did not affect chow consumption, but increased grain pellet consumption (*** $p \leq 0.001$, Mann-Whitney U test).
(H-K) Wild-type mice with rimonabant injection.
(L-O) *CB1R*$^{lox/lox}$ mice with AAV-Cre-tdTomato injection into the CeA.
(H, J, L, N) Freezing during fear memory acquisition (left) and retrieval during feeding (right).
(I, K, M, O) Average motion index during feeding.
(H-I, L-M) Chow Pellets.
(J-K, N-O) Grain Pellets.
(P) Freezing during fear memory acquisition (left) and retrieval before feeding (right).
(Q) Total distance traveled in the open field during feeding.
(R) Latency to reach to cup (left), initial feeding (middle) and (feed - cup) (right).
(S) Percentage of time spent in each zones of the open field during feeding.
Statistics: no significant differences in all figures except G (grain). Also see Table S1.